Eur. Phys. J. Plus (2024) 139:791
https://doi.org/10.1140/epjp/s13360-024-05225-9

THE EUROPEAN PHYSICAL JOURNAL PLUS

Regular Article

Assessment of impurity production upon 14 MeV fusion neutron irradiation of both natural and isotopically enriched ^{100}Mo samples

S. Palomba[1,a], G. Dellepiane[2], R. Falconi[3], R. Faccini[3], A. Fazio[4,5], M. Capogni[4,5], M. Capone[4,5], A. Colangeli[4], P. De Felice[4,5], A. Vannozzi[6], A. Pietropaolo[4]

[1] Department of Industrial Engineering, University of Roma Tor Vergata, Rome, Italy
[2] Albert Einstein Centre for Fundamental Physics (AEC), Laboratory for High Energy Physics (LHEP), University of Bern, Bern, Switzerland
[3] La Sapienza University of Rome, Rome, Italy
[4] ENEA - Department of Fusion and Technologies for Nuclear Safety and Security, Rome, Italy
[5] ENEA-Italian National Institute of Ionizing Radiation Metrology, Rome, Italy
[6] ENEA-FSN-Superconductivity Section, Frascati, Italy

Received: 25 November 2022 / Accepted: 17 April 2024

Abstract ^{99m}Tc, a decay product of ^{99}Mo, is the most widely used radionuclide in single photon emission computed tomography (SPECT). Currently, ^{99}Mo is mainly produced by nuclear reactors as isotope separation from fission products by ^{235}U-enriched (HEU or LEU) uranium targets. Due to problems related to the ageing of nuclear fission reactors, new techniques are presently taken into consideration. In this paper, the ^{99}Mo production based on the ^{100}Mo(n,2n)^{99}Mo reaction route, using 14 MeV fusion neutrons, is investigated. To this end, two samples were tested, manufactured as natural molybdenum metallic powder encapsulated in a container and ^{100}Mo-enriched molybdenum metallic pellet, respectively. The main goal of the experimental investigation was to determine the isotope inventory, as well as the amount of impurities generated in the neutron-irradiated samples. The experimental results were compared to numerical calculations obtained by means of MCNP and FISPACT-II codes. A prediction of the expected activity of ^{99}Mo under the aforementioned irradiation conditions is also provided for the future high-brilliance 14 MeV neutron source named SORGENTINA-RF.

1 Introduction

The research and development of ^{99}Mo production pathways, alternative or complementary to current nuclear fission reactors, is strategic in the mid-to-long-term. After the global crisis occurred in 2009/2010 [1, 2], mostly caused by the ageing of the main fission reactors authorized to ^{99}Mo production, the scientific community was asked to investigate different supply routes, not only alternative to reactors (because of ageing) but also to the use of ^{235}U to avoid the proliferation of nuclear weapon grade materials [3, 4]. In the framework of the international efforts underway, a series of experiments as well as theoretical calculations were performed based upon the use of 14 MeV fusion neutrons to produce ^{99}Mo via the ^{100}Mo(n,2n)^{99}Mo reaction route [5–7]. Such a feasible reaction route has been defined by the Organisation for Economic Co-operation and Development (OECD) as one of the possible long-term solutions aimed at producing ^{99}Mo in the scenario that keeps the current supply technology unchanged [4]. A series of investigations were carried out at ENEA (The Italian National Agency for energy, Environment and Sustainable economic development), thanks to a synergic activity between the Frascati neutron generator (FNG) facility and the Italian National Institute for Ionizing radiation metrology (INMRI), where irradiation experiments on both natural and ^{100}Mo-enriched metallic samples, and ^{99}Mo activity measurements as well as impurities determination assessment were conducted, respectively [9]. This goal of this study is in particular focused on the impurities determination in a natural molybdenum sample and the degree of purity of the pertechnetate solution obtained from ^{100}Mo-enriched molybdenum sample, upon neutron irradiation at 14 MeV. Such measurements were used to benchmark numerical calculations which, in turn, were used to estimate the impurity level expected at a high intensity 14 MeV fusion neutron source.

[a] e-mail: silvia.palomba@uniroma2.it (corresponding author)

Published online: 06 September 2024

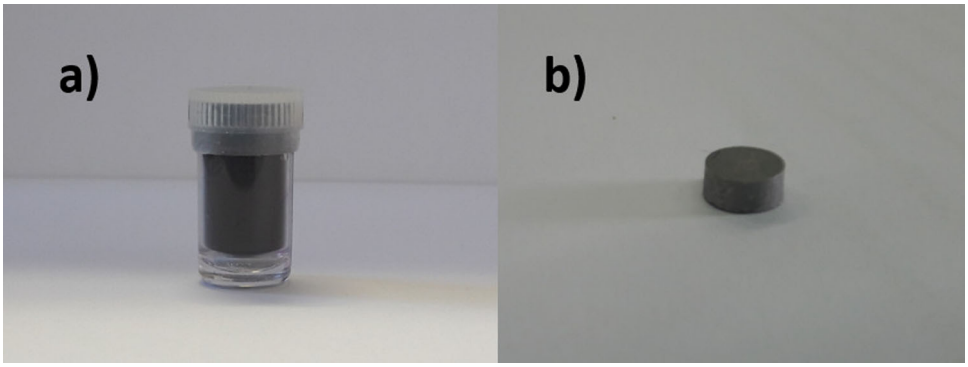

Fig. 1 **a** ^{nat}Mo powder in a plastic container. **b** Cylindrical sintered ^{100}Mo pellet from ISOFLEX

Table 1 Isotopic composition of the ^{nat}Mo [8] metallic powder used

Isotope	^{92}Mo	^{94}Mo	^{95}Mo	^{96}Mo	^{97}Mo	^{98}Mo	^{100}Mo
Concentration (%)	15.86	9.12	15.70	16.50	9.45	23.75	9.62

Table 2 Isotopic composition of the ^{100}Mo-enriched by ISOFLEX

Isotope	^{92}Mo	^{94}Mo	^{95}Mo	^{96}Mo	^{97}Mo	^{98}Mo
Concentration (%)	0.06	0.03	0.04	0.05	0.08	0.47

Table 3 List of elemental impurities in the ^{100}Mo-enriched pellet provided by ISOFLEX

Element	Mn	Cr	Cu	Fe	Sn	Ni	Si	Na	Mg	Ti	Al	Co	Zn	W
Concentration (ppm)	1	1	10	20	1	1	70	1	5	20	20	1	1	<100

2 Experimental set-up

2.1 Samples preparation and characterization

All the irradiation experiments were performed at the FNG facility [10]. This is an accelerator-driven fusion neutron source relying on a 1 mA current-300 keV energy deuteron beam impinging on a thin deuterated/tritiated target.

The nominal neutron emission rate in D-D and D-T mode is 10^9 s^{-1} and 10^{11} s^{-1}, respectively.

In what follows, a description of the samples used and characterization procedures adopted is shown. Two different samples, shown in Fig. 1, were irradiated by 14 MeV neutrons, namely:

- ^{nat}Mo metallic powder having mass of (4.88585 ± 0.00001) g placed inside a cylindrical plastic container measuring 2.1 cm in height and 1.2 cm in diameter (Fig. 1a). In Table 1, the isotopic composition of it is shown;
- a 0.4 cm thickness, 0.6 cm diameter cylindrical pellet (Fig. 1b) of sintered ^{100}Mo-enriched (99.27%) metallic powder, with a mass (0.80503 ± 0.00001) g produced by ISOFLEX USA. In Table 2 the isotopic composition of it is shown. In Table 3 the list of elemental impurities composition in the enriched target is shown, as reported by the ISOFLEX documents.

To verify the impurity presence in samples prior irradiation, a further elemental analysis by X-ray diffraction measurements was carried out at the ENEA-Frascati superconductivity laboratory.

2.2 Elemental analysis

The elemental analysis was performed by means of energy-dispersive spectroscopy (EDS) using an Oxford X-act SDD 129 eV detector, mounted on a Leo 1525 scanning electron microscope. Spectra were analysed using the AZtec v. 3.2 HF1 software. Figure 2 shows the EDS spectra of the ^{nat}Mo powder and the sintered ^{100}Mo pellet. The relatively high oxygen peak in Fig. 2a is consistent with the very high surface area of powders. Sintering is effective in removing surface oxidation (Fig. 2b). The presence of Fe and Cr is probably due to the remains of the pressing for the formation of the pellet.

2.3 X-ray diffraction

The X-ray diffraction was carried out using a Rigaku Geigerflex diffractometer, in Bragg-Brentano configuration, working with Cu-Kα radiation equipped with a curved graphite crystal monochromator on the diffracted beam in order to increase the signal-to-noise

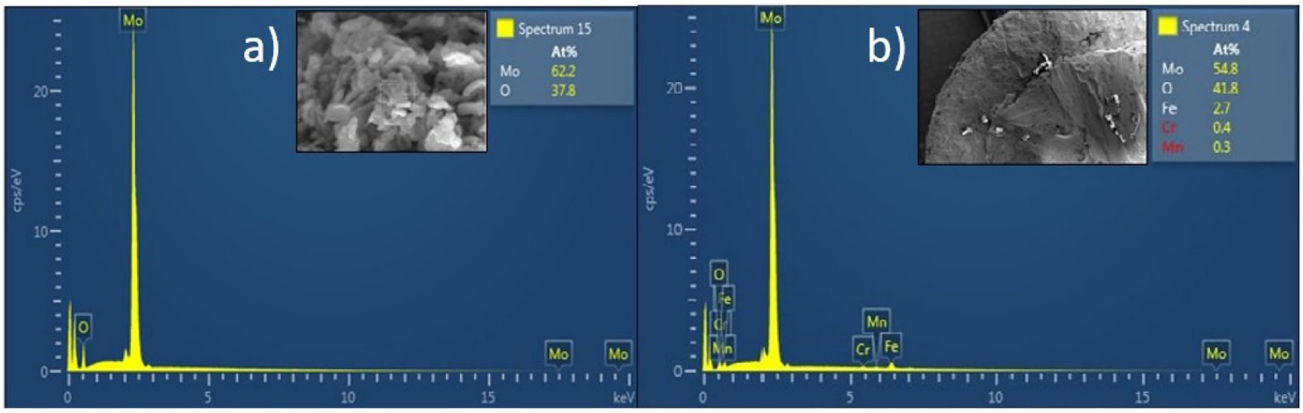

Fig. 2 **a** EDS spectrum of ^{nat}Mo powder. **b** EDS spectrum of sintered ^{100}Mo pellet. The photos show the areas of the samples analysed with X-rays

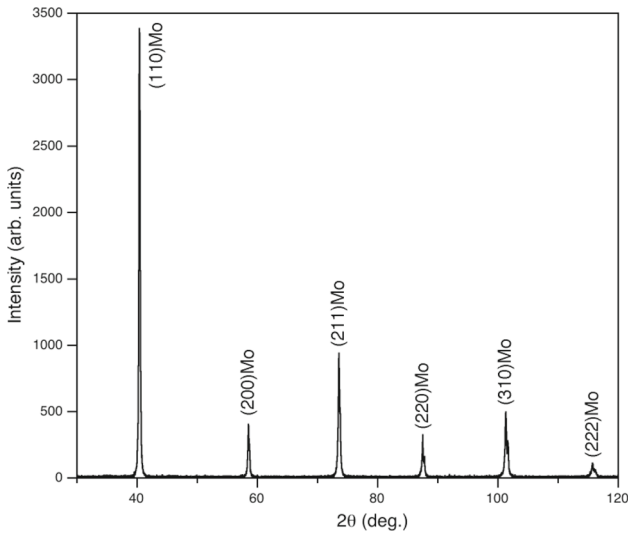

Fig. 3 X-ray diffraction pattern of the ^{100}Mo sintered pellet

ratio and to remove Cu-Kβ radiation. Figure 3 shows the $\theta - 2\theta$ spectrum of ^{100}Mo pellet. Only peaks related to Mo element can be seen. The intensity ratios of the peaks are in good agreement with reference data [11].

3 Samples irradiation set-up

FNG is an accelerator-driven, continuous mode, fusion neutron source. It relies on a deuteron accelerator of about 300 W power (300 keV energy and up to 1 mA current). The beam is directed toward a copper substrate layered by 4 μm thickness of titanium, where tritium or deuterium is implanted. Depending upon the needs, this allows to produce either 2.5 MeV or 14 MeV neutrons by exploiting the ^{2}H(^{2}H,n)^{3}He and the ^{2}H(^{3}H,n)^{4}He reactions, respectively [10].

Fig. 4 shows the sample holder used for the irradiation, while Fig. 5 shows the experimental set-up for the powder and the pellet samples. The distance from the target to the centre of the sample is (3.3 $\pm$ 0.1) cm and (3.1 $\pm$ 0.1) cm for ^{nat}Mo powder container and ^{100}Mo-enriched sintered pellet, respectively.

The ^{nat}Mo powder irradiation was performed at a neutron source rate of 2.0$\times$ 10^{10} s^{-1} and over an irradiation time of 5400 s (i.e. 1h, 30 min). About the ^{100}Mo pellet, the neutron source rate was 3.56$\times$ 10^{10} s^{-1} and the irradiation time lasted 3360 s (i.e. 56 min).

In order to calculate the ^{99}Mo yield expected as well as the impurities inventory produced, the MCNP5 v1.6 [12] Monte Carlo code was used to simulate the neutron irradiation experiment at FNG. For this purpose, the irradiation set-up was modelled in MCNP [13]. Figures 6 and 7 show the neutron spectral fluence rate as determined by MCNP simulation and the geometric reconstruction of the natural Mo powder and the enriched ^{100}Mo pellet, respectively.

After neutron irradiation, the activation level of the samples was measured by using a high purity germanium (HPGe) gamma spectrometer. Figure 8 shows the pulse-height distribution recorded a few minutes after irradiation (EOI).

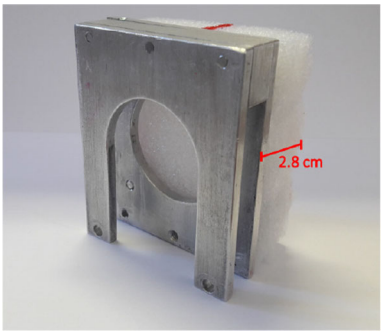

Fig. 4 The support used for samples irradiation at the FNG facility

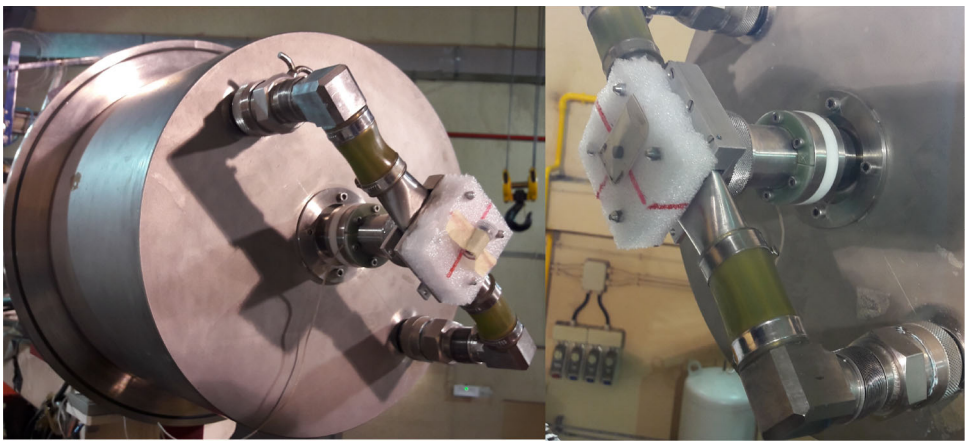

Fig. 5 Positioning of the ^{nat}Mo powder (left panel) and the ^{100}Mo pellet (right panel) in front of the FNG target

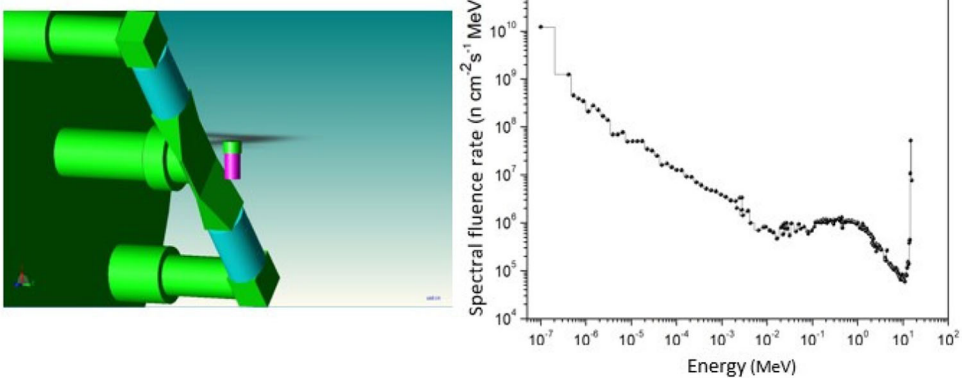

Fig. 6 3D MCNP geometry model for the irradiation of ^{nat}Mo powder sample (left panel) and neutron spectral fluence rate at the sample position calculated by MCNP (right panel)

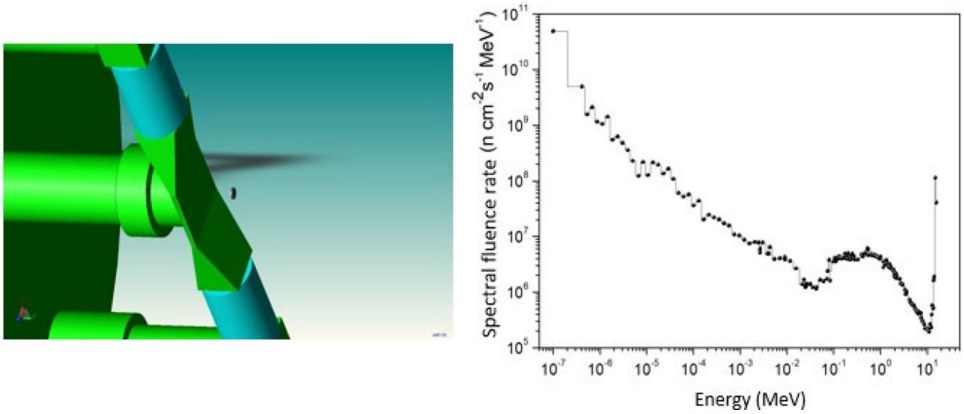

Fig. 7 3D MCNP geometry model for the irradiation of ^{100}Mo pellet (Left panel) and neutron spectral fluence rate at the sample position calculated by MCNP (Right panel)

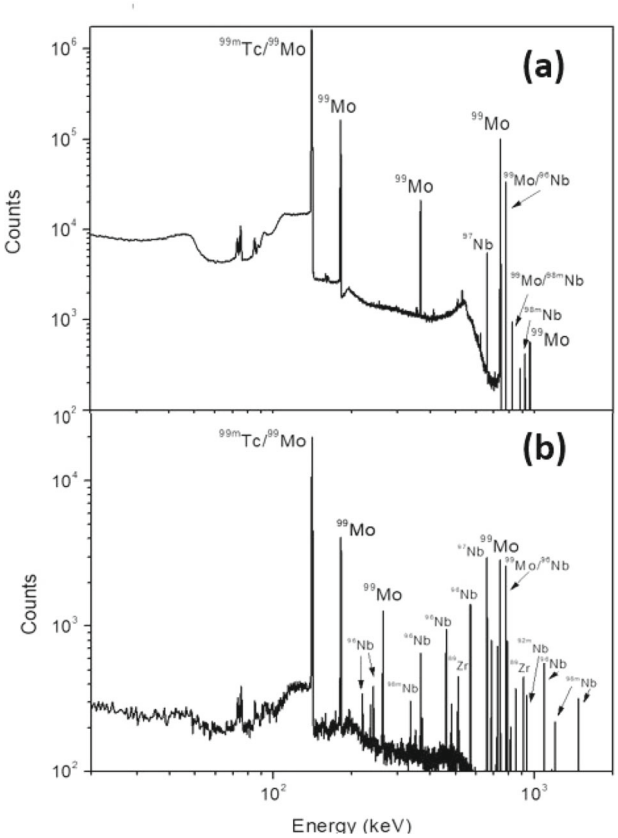

Fig. 8 Pulse-height spectrum of the ^{100}Mo pellet (**a**) and of the ^{nat}Mo powder sample (**b**), after 14 MeV neutron irradiation (EOI) measured using an HPGe detector in the INMRI laboratories

4 Molybdate preparation

Both powder and pellet were subject to a radiochemical process to obtain the molybdate solution ($^{99}MoO_4^{2-}$). For this purpose, 35 ml of hydrogen peroxide at 30% w/v of concentration and 25 ml of sodium hydroxide at 8 mol/L were added to ^{nat}Mo powder. To reduce the volume of solution at 4 ml, the volume of the vial used for gamma spectrometry, molybdate solution was reduced to a small volume with a heating plate.

The solution obtained starting from ^{nat}Mo is composed not only by molybdate, but containing impurities, as well.

For the ^{100}Mo pellet, a preliminary dissolution with *Aqua Regia* (HNO_3/HCl 1:3 v/v) was necessary. After complete digestion, the solution was heated until it reduces to dryness and then H_2O_2 at 30% w/v and NaOH at 8 mol/L were added. In this case the pertechnetate solution was separated from the molybdate solution. The extraction technique used is the one making use of the MethylEthylKetone (MEK) solvent [14]. The solvent was added to the aqueous solution binding with the pertechnetate ($^{99m}TcO_4^-$); since, the solvent was non-mixable in inorganic solutions, with a separating funnel, the two phases were separated. At last, 4 ml of pertechnetate solution were used to measure the ^{99m}Tc resulting activity.

5 Activity measurements at ENEA-INMRI

The activity measurements were carried out at the Radioactivity Laboratory of the ENEA-INMRI under high-metrological conditions [15]. A high-resolution HPGe spectrometer (ORTEC GEM40-83-S9), calibrated with high-level metrological standards available at the Institute, was used to measure the yielded activities of the irradiated samples. After the radiochemical procedures, impurity analysis of molybdate and ^{99m}Tc activity measurements were carried out.

As far as the molybdate solution obtained from ^{nat}Mo is concerned, the impurity analysis was performed at $t = 0$ (EOI) and at $t = 12$ hours, which corresponds to the typical transport time from the processing site to radiopharmacies. Actually, the activity of the molybdate solution was measured 24 h after the end of irradiation, but the activity at earlier times were dated back by using the law of radioactive decay.

Regarding the pertechnetate solution obtained by the ^{100}Mo pellet irradiation, the activity of ^{99m}Tc was determined by gamma spectrometry analyses. Figure 9 shows pulse-height spectrum of pertechnetate solution.

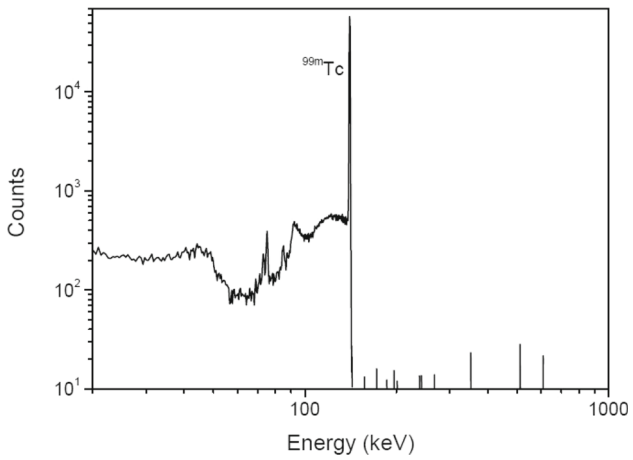

Fig. 9 Pulse-height spectrum of the perthecnetate recorded by means of a HPGe detector at the ENEA-INMRI laboratory

Table 4 List of possible reaction routes among 14 MeV neutrons and molybdenum isotopes (^{nat}Mo/^{100}Mo-enriched molybdenum)

Father isotope	Reaction	Dauther radionuclide
^{92}Mo	(n,α)	^{89m}Zr
^{100}Mo		^{97}Zr
^{92}Mo	(n,2n)	^{91m}Mo
^{100}Mo		^{99}Mo
^{92}Mo	(n,p)	^{92m}Nb
^{94}Mo		^{94m}Nb
^{95}Mo		^{95m}Nb
^{96}Mo		^{96}Nb
^{97}Mo		^{97m}Nb
^{98}Mo		^{98m}Nb
^{100}Mo		^{100m}Nb
^{92}Mo	(n,γ)	^{93m}Mo
^{100}Mo		^{101}Mo
^{92}Mo	(n,np)	^{91m}Nb
^{94}Mo	(n,nα)	^{90m}Zr
^{96}Mo	(n,d)	^{95m}Nb

6 Discussion

In Table 3, all the possible nuclear reaction routes that can occur among the different molybdenum isotopes (both in natural and enriched targets) and 14 MeV source neutrons are enlisted.

FISPACT-II code calculates the activities of the produced radionuclides and related decay chains by using the well-known set of Bateman's equations of radioactive decay law.

In order to perform the calculation, FISPACT-II makes use of the neutron fluence, provided by the MCNP code. In such a way, it was possible to calculate the activity of the whole inventory of radionuclides at different times after EOI.

As FISPACT-II calculation at t= 12 h was made on ^{99}Mo, while the analysis carried out at ENEA-INMRI was on the molybdate solution, it was verified that the radiochemical procedure did not result in changes in the radionuclidic composition of the sample; it was therefore possible to compare the two results.

The results of the study at t=0 and t=12 h are shown in Tables 5 and 6, respectively, with the ratio of the activity fraction to the total activity.

In addition to the radionuclide activities, Tables 5 and 6 also show the ratio of the activity fraction to the total activity measured in the sample (A_{kX}/A_{tot}), expressed as a percentage.

It is worth to highlight that some activity values that are calculated by FISPACT-II are lower than the minimum detectable activity (MDA) of the HPGe, such as the ^{95}Zr, ^{95m}Nb, ^{97}Nb and ^{98m}Nb.

As previously stated, the gamma spectrometry measurement at ENEA-INMRI has started 24 h after EOI. As ^{99m}Tc has one emission line at 140.51 keV, which it shares with ^{99}Mo, and its activity is close to zero at EOI, a comparison was carried out between

Table 5 The ratio of the radionuclide's activity to the total activity (A_{kX}/A_{tot}) and the activity of radionulides calculated at t =0 after irradiation (EOB), in ^{nat}Mo powder by FISPACT-II calculations and rescaled by gamma spectrometry measurements in molybdate by ENEA-INMRI analyses

Radionuclide	$t_{1/2}$	FISPACT-II		INMRI	
		A_{kX}/A_{tot} (%)	Activity (Bq)	A_{kX}/A_{tot} (%)	Activity (Bq)
^{99}Mo	65.94 h	50.46	5252 ± 314	86.06	4360 ± 360
^{93m}Mo	6.85 h	2.45	255±39	2.70	137 ± 35
^{92m}Nb	243.6 h	40.92	82 ± 14	1.44	73 ± 8
^{96}Nb	23.35 h	4.16	433 ± 92	7.09	359 ± 28
^{97}Nb	72.1 min	0.79	4259 ± 1518	0.79	40 ± 8
^{89}Zr	78.41 h	1.22	127 ± 12	1.91	97 ± 11

Table 6 The ratio of the radionuclide's activity to the total activity (A_{kX}/A_{tot}) and the activity of radionulides calculated at t =12 h after irradiation (EOB), in ^{nat}Mo powder by FISPACT-II calculations and rescaled by gamma spectrometry measurements in molybdate by ENEA-INMRI analyses

Radionuclide	$t_{1/2}$	FISPACT-II		INMRI	
		A_{kX}/A_{tot} (%)	Activity (Bq)	A_{kX}/A_{tot} (%)	Activity (Bq)
^{99}Mo	65.94 h	87.65	4630 ± 277	88.31	3843.4 ± 317.7
^{93m}Mo	6.85 h	0.70	76±12	0.94	41 ± 10
^{95}Nb	34.98 d	0.21	23 ± 6	0.32	14 ± 3
^{92m}Nb	10.15 d	0.73	79 ± 14	1.63	71 ± 8
^{96}Nb	23.35 h	2.80	303 ± 64	5.77	251 ± 20
^{97}Nb	1.20 h	0.29	31 ± 11	0.55	24 ± 5
^{89}Zr	78.41 h	1.07	116 ± 12	2.02	88 ± 9
^{97}Zr	16.91 h	0.22	24 ± 4	0.46	20 ± 4

Table 7 ^{99m}Tc activity in ^{nat}Mo powder by FISPACT-II calculations and rescaled by gamma spectrometry measurements in molybdate by ENEA-INMRI analyses

	FISPACT-II	INMRI
Radionuclide	A_2(t) (Bq)	A_2(t) (Bq)
^{99m}Tc	(3189 ± 323)	(3310 ± 256)

Table 8 The activity fraction to the total activity (A_{kX}/A_{tot}) and the activity of other radionuclides present at t =0 after irradiation, of ^{nat}Mo as calculated by FISPACT-II

Radionuclide	$t_{1/2}$	A_{kX}/A_{tot} (%)	Activity (Bq)
^{91}Mo	2.58 h	73.86	87838 ± 10497
^{101}Mo	2.44 h	0.40	472 ± 158
^{91m}Mo	64.6 h	10.15	12072 ± 1820
^{97m}Nb	1.08 min	1.63	1944 ± 1645
^{94m}Nb	6.26 min	9.20	10945 ± 7131
^{100m}Nb	2.99 s	0.25	303 ± 193
^{98}Nb	2.86 s	3.25	3869 ± 2524
^{100}Nb	1.5 s	0.36	432 ± 272
^{101}Tc	14.02 min	0.38	448 ± 149
^{90m}Zr	0.8 s	0.40	481 ± 361
^{89m}Y	15.7 s	0.11	126 ± 45

FISPACT-II and HPGe at a time of 24 h, i.e. the measurement time. The activity of ^{99m}Tc radionuclides, A_2(t), present after 24 h from irradiation in molibdate solution, is experimentally determined and compared to that calculated by FISPACT-II, see Table 7.

Tables 8 and 9 show the radionuclides found in the activated ^{nat}Mo sample, at t=0 and t=12 h, respectively, calculated by FISPACT-II. In particular, the radionuclides shown in the Table 8 have a half-life of less than 4.8 h, and therefore were completely decayed at the time of the gamma spectrometry measurements. While, the radionuclides present in the table mostly have a low probability of gamma emission or, like ^{91}Nb, have a β^+-decay that is difficult to distinguish in the peak at 511 keV.

These radionuclides were not detected by HPGe of ENEA-INMRI, because their activity was lower than the MDA due to the interplay of low intensity of the neutrons source and the short irradiation time. These radionuclides would have been detectable if the samples were irradiated with a higher neutron intensity, as that foreseen for the SORGENTINA-RF neutrons source [17].

Table 9 The activity fraction to the total activity (A_{kX}/A_{tot}) and the activity of other radionulides present at t =12 h after irradiation, of ^{nat}Mo as calculated by FISPACT-II calculations

Radionuclide	$t_{1/2}$	A_{kX}/A_{tot} (%)	Activity (Bq)
^{91}Nb	678.59 yr	$9.14{\cdot}10^{-4}$	$5.05{\cdot}10^{-2}$
^{93m}Nb	16.14 yr	$3.31{\cdot}10^{-4}$	$1.83{\cdot}10^{-2}$
^{95m}Nb	3.60 d	0.69	38 ± 11
^{91m}Nb	60.86 d	1.19	66 ± 14
^{88}Zr	83.4 d	$9.14{\cdot}10^{-5}$	$5.05{\cdot}10^{-3}$

Table 10 ^{99}Mo specific activity measured at ENEA-INMRI Laboratory and normalized to the neutrons source rate of FNG facility, $A_{sN}(t)$

	$A_{sN}(t) \cdot 10^{-11}$ kBq s/g
^{nat}Mo	(5.01 ± 0.04)
^{100}Mo	(50 ± 2)

In the analysis carried out on the 100Mo-enriched target sample, the main focus was to evaluate the activity of ^{99m}Tc. Also in this case the experimental data were compared with the FISPACT-II predictions, since the radiochemical procedure did not make any specific changes to the radionuclide composition of pertechnetate solution.

A further comparison was made between the ^{99}Mo specific activity, $A_s(t)$, measured by the ENEA-INMRI HPGe detector normalized to the neutrons source rate at 14 MeV, Table 10 shows the results, intercepted by the sample over the irradiation time, for the natural molybdenum powder and ^{100}Mo-enriched sample.

7 Conclusions

The method of ^{99}Mo production using the ^{100}Mo(n,2n)^{99}Mo reaction route was investigated. Mo samples were irradiated at the FNG facility and the produced activities were measured at the INRMI-ENEA Laboratory.

The main objective of the experimental investigation was to determine the type and the amount of impurities generated in the neutron-irradiated samples and how these are eventually transported during the radiochemical processing the final production of the radiopharmaceutical. This was made by irradiating two different samples: ^{nat}Mo powder and ^{100}Mo pellet. From the comparison between the experimental results from ENEA-INMRI and MCNP-FISPACT-II codes calculations it can be stated that in the molybdate solution from ^{nat}Mo the impurities are:

- Belonging to the molybdenum family: the ^{91m}Mo, the ^{93m}Mo and the ^{101}Mo;
- Belonging to the zirconium family: the ^{95}Zr, the ^{97}Zr, the ^{89m}Zr and the ^{90m}Zr;
- Belonging to the niobium family: the ^{91}Nb, the ^{93m}Nb, the ^{92m}Nb, the ^{94}Nb, the ^{95}Nb, the ^{95m}Nb, the ^{96}Nb, the ^{97m}Nb and the ^{98m}Nb, the ^{95m}Nb;
- Belonging to the yttrium family: ^{89}Y.

The determination of the impurities is important for the transportation of the irradiated material from the production site to the radiochemical laboratory. Furthermore, it is of paramount importance in order to define the important to define the chemical strategy to be adopted in the purification phase. The perthecnetate solution extracted with the MEK from the molybdate solution obtained from ^{100}Mo is pure as no other radionuclides were found.

The main advantages of producing ^{99}Mo by using of 14 MeV neutrons are:

- The molybdate solution obtained from ^{nat}Mo is purer than the solution obtained with a ^{99}Mo obtained by ^{235}U fission.
- From the radiochemical point of view the pertechnetate solution is pure. Biological purity was not experimentally assessed at this stage.

Acknowledgements The author acknowledge Dr. M. Pillon and Dr. S. Loreti (from ENEA-FNG) for useful discussions.

Funding Open access funding provided by Università degli Studi di Roma Tor Vergata within the CRUI-CARE Agreement.

Data Availability Statement The data sets generated during and/or analysed during the current study are available from the corresponding author on reasonable request. The manuscript has associated data in a data repository.

References

1. P. Gould, Nature **460**, 312 (2009)
2. R. Van Noorden, Nature **504**, 202 (2013)
3. D.L. Bailey, J.L. Huum, A. Todd-Pokropek, A. Van Aswegen et al., *Nuclear Medicine Physics: A Handbook for Teachers and Students* (International Atomic Energy Agency (IAEA), Vienna, 2014)
4. OECD Nuclear Energy Agency, *NEA-OECD, Report on the Supply of Medical Radioisotopes: An Assessment of Long-Term Global Demand for Technesium-99m* (OECD, Paris, 2011)
5. A. Pietropaolo, M. Capogni, L. Quintieri, Nature **603**, 393 (2022). https://doi.org/10.1038/d41586-022-00705-3
6. M. Capogni et al., Molecules **23**, 1872 (2018)
7. M. Capogni et al., Appl. Rad. Isotop. **134**, 105 (2018)
8. Cooke, D. R., et al. Geochemistry of porphyry deposits. (2014)
9. M. Capogni, A. Pietropaolo, L. Quintieri, *^{99m}Tc production via ^{100}Mo(n,2n)^{99}Mo reaction using 14 MeV neutrons from a D-T neutron source: Discussion for a scientific case, RT/2016/32/ENEA* (Roma, Italy, ENEA, 2016)
10. M. Martone, M. Angelone, M. Pillon, Jour. Nucl. Mater. **212**, 1661 (1994)
11. JCPDS Powder Diffraction Data, International Centre for Diffraction Data (1997) card no. 42-1120
12. X-5 Monte Carlo Team: MCNP - A General Monte Carlo N-Particle Transport Code, Version 5, LANL Report LACP-03-0245
13. M. Pillon, M. Martone, M. Angelone, Technical Report rt/eng/fus/93/65, (1995), Frascati-ENEA
14. P. Martini et al., A Solvent-Extraction Module for Cyclotron Production of High-Purity Technetium-99m, Applied Radiation and isotopes, Volume 118, **302-307**, (2016) https://doi.org/10.1016/j.apradiso.2016.10.002
15. https://www.inmri.enea.it/en/
16. M. Fleming ,T. Stainer ,M. Gilbert, FISPACT-II User Manual. Tech. Rep. UKAEA-R(18)001UKAEA (2018) URL :http://fispact.ukaea.uk/
17. A. Pietropaolo et al., Europ. Phys. J. Plus **136**(11), 1140 (2021)